Influence of doping on the dielectric function in narrow-gap semiconductors

Qian Dingrong
National Laboratory for Infrared Physics, 420 Zhong Shan Bei Yi Road, Shanghai 200 083, China

L. Liu
Department of Physics, Northwestern University, Evanston, Illinois 60201

W. Szuszkiewicz
Institute of Experimental Physics, Warsaw University, Hoza 69, 00-681 Warsaw, Poland

W. Bardyszewski
Institute of Theoretical Physics, Warsaw University, Hoza 69, 00-681 Warsaw, Poland
(Received 6 April 1990; revised manuscript received 29 January 1991)

The influence of doping on the intraband Lindhard dielectric functions of free carriers in narrow-gap semiconductors has been studied at zero temperature using a geometric approach in momentum space for two extreme cases, i.e., light and heavy doping corresponding to parabolic and linear energy bands, respectively. In the case of heavy doping, the dielectric function turns out to be different, and free carriers also behave differently, showing no coupling between single-carrier transitions and the collective excitations of the carriers. This accounts well for the experimental results measured on an In-doped $Hg_{1-x}Cd_xTe$ sample reported previously.

I. INTRODUCTION

The response of a many-electron system to an external perturbation can be discussed most generally in terms of a frequency- and wave-number-dependent dielectric function $\epsilon(\mathbf{q},\omega)$. This is a very important quantity because it contains a great deal of information about the properties of the electron system in addition to the system's response to external probes. Under certain circumstances, when only the effect of $q \to 0$ or $\omega \to 0$ are needed, the task becomes considerably simpler. In one limit, $\epsilon(\mathbf{q},0)$ describes the electrostatic screening of the electron-electron, electron-lattice, and electron-impurity interaction in crystals and can be used to study the effect of these screenings on free carrier scattering in transport phenomena as well as in free carrier absorption in semiconductors. In another limit, $\epsilon(0,\omega)$ describes the collective excitation of the Fermi sea, i.e., the volume and surface plasmons. The purpose of this paper is to calculate the dielectric function in the region between the two limiting cases, i.e., a region of infrared and rather long wavelengths, for narrow-gap semiconductors of which the energy bands are described by Kane's model.[1] However, the actual evaluation of $\epsilon(\mathbf{q},\omega)$ even in the framework of random-phase approximation is generally very difficult; if the system under consideration is other than a free-electron gas, one has to deal with the many-body problem of a gas of electrons interacting with each other. These interactions are strong, and are of long range, having the Coulomb force between them and along with the so-called exchange force associated with the antisymmetry of the wave functions. A lot of effort has been expended on the problem of a gas of electrons interacting via their Coulomb potential, and the basic effects of the interaction are now well understood. Much of the theory is expressed in complicated formal language, but the main results are surprisingly simple, and can be derived by elementary arguments.

In a semiconductor, Lindhard's expression[2] for the frequency- and wave-number-dependent dielectric function can be obtained by a simple perturbation theory:[3]

$$\epsilon(\mathbf{q},\omega)=\epsilon_\infty+\frac{4\pi e^2}{q^2}\sum_{\mathbf{q}'}\frac{|\langle \mathbf{q}'|e^{i\mathbf{q}\cdot\mathbf{r}}|\mathbf{q}'+\mathbf{q}\rangle|^2[f^0(\mathbf{q}')-f^0(\mathbf{q}'+\mathbf{q})]}{E(\mathbf{q}'+\mathbf{q})-E(\mathbf{q}')-\hbar\omega+i\hbar\alpha}=\epsilon_\infty+\Delta\epsilon_{\mathrm{intra}}(\mathbf{q},\omega)\ , \quad (1)$$

where $\mathbf{q}$ is the wave vector, α the damping constant, $E(\mathbf{q})$ the energy eigenvalue at state $\mathbf{q}$, $|q\rangle$ the corresponding eigenvector, and $f^0(\mathbf{q})$ distribution function, respectively. ϵ_∞ is the contribution due to all interband transitions, which is, strictly speaking, complex, but at low temperatures the imaginary part goes to zero in the region where the energy is less than the Fermi level.[4] The contribution from the phonon can be omitted if its frequency is much less than the frequency region of interest. The matrix element represents an overlap between the spatially periodic part of the two Bloch functions, so it is accurate enough for free electrons in narrow-gap semiconductors to take it as a unit.

Taking into account the property of δ functions,

$$\lim_{\alpha\to 0}\frac{1}{x-x_0+i\alpha}=\mathrm{P}\frac{1}{x-x_0}-i\pi\delta(x-x_0)\ , \tag{2}$$

where P denotes the principal part. The imaginary part of the dielectric function given in Eq. (1) can then be obtained from Eq. (2):

$$\Delta\epsilon''_{\mathrm{intra}}(\mathbf{q},\omega)=-\frac{4\pi^2e^2}{q^2}\sum_{\mathbf{q}'}[f^0(\mathbf{q}')-f^0(\mathbf{q}'+\mathbf{q})]\times\delta(E(\mathbf{q}'+\mathbf{q})-E(\mathbf{q}')-\hbar\omega)\ . \tag{3}$$

For the purpose of calculation, substitution can be made:

$$\sum_{\mathbf{q}'}\to\frac{2}{(2\pi)^3}\int_0^{\infty}\int_{+1}^{-1}\int_0^{2\pi}(q')^2dq'd\mu\, d\phi\ , \tag{4}$$

where $\mu=\cos\theta$ and $\theta\angle(\mathbf{q}',\mathbf{q})$.

At absolute zero temperature, Eq. (3) gives

$$\Delta\epsilon''_{\mathrm{intra}}(\mathbf{q},\omega)=\frac{4\pi^2e^2}{q^2}\frac{2}{(2\pi)^3}\int_0^{k_F}\int_{-1}^{1}\int_0^{2\pi}(q')^2\delta(E(\mathbf{q}'+\mathbf{q})-E(q')-\hbar\omega)dq'd\mu\, d\phi\ , \tag{5}$$

where k_F is the wave vector at the Fermi surface and $E(\mathbf{q})$ is the energy of a free carrier in a semiconductor described by the Kane model in the case of narrow-gap semiconductors, namely,

$$E(q)=\tfrac{1}{2}[(E_g^2+\tfrac{8}{3}q^2P^2)^{1/2}-E_g]\ , \tag{6}$$

where P is the element of momentum matrix and E_g is the energy gap at the Γ point between Γ_6 and Γ_8. The algebraic calculation of Eq. (5) for the linear band was previously performed by Szuszkiewicz and Bardyszewski.[5]

II. LIGHT DOPING (PARABOLIC BAND)

All states are at the bottom of the conduction band $E_g \gg kP$. It is seen from Eq. (6) that the energy dispersion relation is parabolic:

$$E(q)=\frac{\hbar^2q^2}{2m^*},\quad m^*=\frac{3\hbar^2E_g}{4P^2}\ . \tag{7}$$

In this case, Eq. (5) turns out to be

$$\Delta\epsilon''_{\mathrm{intra}}(\mathbf{q},\omega)=\frac{4\pi^2e^2}{q^2}\frac{2}{(2\pi)^3}\int_0^{k_F}\int_{-1}^{1}\int_0^{2\pi}(q')^2\delta\left[\frac{\hbar^2}{2m^*}(q^2+2q'q\mu)-\hbar\omega\right]dq'd\mu\, d\phi\ . \tag{8}$$

The integral is to be carried out in the volume outside the left Fermi sphere and inside the right Fermi sphere in k space (Fig. 6). However, because of the δ function, which sets a confinement for q' and θ, they are not independent any longer; the volume integral then reduces to a surface integral on a disk or ring depending on the value of q' and ω. It is known from Appendix A that (a) when $0<\hbar\omega<-(\hbar^2/2m^*)(q^2-2qk_F)$ [equivalent to $q+\mathbf{q}'\cdot\mathbf{q}<k_F$, from Eq. (A2)],

$$q'_1(\theta_1)=k_F\ ,\qquad q'_2(\theta_2)=(k_F^2-q_\omega^2)^{1/2}=\left[k_F^2-\frac{2m^*\omega}{\hbar}\right]^{1/2}, \tag{9}$$

and (b) when $0<-(\hbar^2/2m^*)(q^2-2qk_F)<\hbar\omega<(\hbar^2/2m^*)(q^2+2qk_F)$ (equivalent to $k_F<q+\mathbf{q}'\cdot\mathbf{q}<q+k_F$),

$$q'_1(\theta_1)=k_F\ ,\qquad q'_2(\theta_2)=\frac{q_\omega^2-q^2}{2q}=\frac{m^*\omega}{\hbar q}-\frac{q}{2}\ . \tag{10}$$

From Eqs. (8), (9), and (10) one has

$$\Delta\epsilon''_{\rm intra}(\mathbf{q},\omega)=\frac{2e^2}{q^2}\int_{q_2'(\theta_2)}^{q_1'(\theta_1)}\frac{m^*q'}{\hbar^2 q}dq'$$
$$=\frac{e^2m^*}{\hbar^2q^3}\{[q_1'(\theta_1)]^2-[q_2'(\theta_2)]^2\}$$
$$=\begin{cases}\dfrac{2e^2(m^*)^2\omega}{\hbar^3q^3} & \text{when } 0<\hbar\omega<-\dfrac{\hbar^2}{2m^*}(q^2-2qk_F)\\[2ex] \dfrac{e^2m^*k_F^2}{\hbar^2q^3}\left[1-\left[\dfrac{\omega m^*}{\hbar qk_F}-\dfrac{q}{2k_F}\right]^2\right] & \text{when } 0<-\dfrac{\hbar^2}{2m^*}(q^2-2qk_F)\le\hbar\omega\le\dfrac{\hbar^2}{2m^*}(q^2+2qk_F)\\[2ex] 0 \text{ elsewhere ,}\end{cases} \tag{11}$$

or in a more brief notation,

$$\Delta\epsilon''_{\rm intra}(\mathbf{k},\Omega)=\begin{cases}\dfrac{\alpha r_s\Omega}{8k^3} & \text{when } \dfrac{\Omega}{4k}<1-k\\[2ex] \dfrac{\alpha r_s}{8k^3}\left[1-\left[\dfrac{\Omega}{4k}-k\right]^2\right] & \text{when } |1-k|\le\dfrac{\Omega}{4k}\le 1+k\\[2ex] 0 \text{ elsewhere ,}\end{cases} \tag{12}$$

where $\mathbf{k}=\mathbf{q}/2k_F$, $\Omega=\omega/\omega_f$, $\hbar\omega_f=\hbar^2k_F^2/2m_f^*$, $\alpha=(4/9\pi)^{1/3}$, $a_0=\hbar^2/m^*e^2$, $r_0=(3/4\pi n)^{1/3}$, and $r_s=r_0/a_0$.

The real part can be calculated from Eq. (12) using the well-known Kramers-Kronig transformation, namely,

$$\Delta\epsilon'_{\rm intra}(\mathbf{k},\Omega)=\frac{2}{\pi}\mathrm{P}\int_0^\infty\frac{s\Delta\epsilon''_{\rm intra}(\mathbf{k},s)}{s^2-\Omega^2}ds\ . \tag{13}$$

Only those terms in Eqs. (11) and (12) that are odd with respect to frequency give nonvanishing results.[6] Substituting Eq. (12) into Eq. (13) yields

$$\Delta\epsilon'_{\rm intra}(\mathbf{k},\Omega)=\frac{\alpha r_s}{2\pi k^2}\left\{1+\frac{1}{4k}\left[1-\left[\frac{\Omega}{4k}-k\right]^2\right]\ln\left|\frac{-\Omega/4+k^2+k}{\Omega/4-k^2+k}\right|+\frac{1}{4k}\left[1-\left[\frac{\Omega}{4k}+k\right]^2\right]\ln\left|\frac{\Omega/4+k^2+k}{-\Omega/4-k^2+k}\right|\right\}$$
$$=\frac{\alpha r_s}{2\pi k^2}[1+A(k,\Omega)+B(k,\Omega)]\ , \tag{14}$$

where $A(k,\Omega)$ and $B(k,\Omega)$ refer to the second and the third terms, respectively. Equations (12) and (14) are the expressions for the dielectric function most widely used in the literature. They are the same as in Refs. 7–9 excluding the printing errors there. However, Eq. (14) is only nominally correct in the case of a long wavelength. As a matter of fact, $A(k,\Omega)$ and $B(k,\Omega)$ are close to each other in their absolute values and are opposite in their signs (Fig. 1). Their absolute values increase with the decreasing k, but $A(k,\Omega)+B(k,\Omega)$ remain negative, with an absolute value slightly greater than one. It is seen from the curves in Fig. 1, where the evaluation was performed in double precision, that when k is smaller than 5×10^{-3} ($q<0.01k_F$), the absolute values of $A(k,\Omega)$ and $B(k,\Omega)$ are 6 orders of magnitude higher than $1+A(k,\Omega)+B(k,\Omega)$, which fails to yield an accurate value of $\Delta\epsilon'_{\rm intra}(\mathbf{k},\Omega)$. There is an expression [Eq. (25)] for $\epsilon'(\mathbf{q},\omega)$ in the case of $q\to0$; however, as will be shown, the expression is not accurate enough in the infrared region, so that one needs a suitable expression for the case between $q\to0$ and large q to deal with the long-wavelength case, for example, the plasmon dispersion in the infrared region. To eliminate this error, it is expected that expanding $A(k,\Omega)$ and $B(k,\Omega)$ into a series will enable us to cancel out the terms with large absolute values and opposite signs leaving only the real value. Let $x=\Omega/4k$ and assume $|x-k|>1$, which is always correct for $k<0.1$, even in the infrared region. Then one has

$$A(k,\Omega)=-\frac{1-x^2+2xk-k^2}{2k}\sum_{n=0}^{\infty}\left[\frac{1}{(2n+1)x^{2n+1}}\sum_{I=0}^{\infty}\frac{(2n+1)(2n+2)\cdots(2n+I)}{I!}\left[\frac{k}{x}\right]^I\right]\ , \tag{15}$$

$$B(k,\Omega)=\frac{1-x^2-2xk-k^2}{2k}\sum_{n=0}^{\infty}\left[\frac{1}{(2n+1)x^{2n+1}}\sum_{I=0}^{\infty}(-1)^I\frac{(2n+1)(2n+2)\cdots(2n+I)}{I!}\left[\frac{k}{x}\right]^I\right]\ , \tag{16}$$

$$A(k,\Omega)+B(k,\Omega)=-\sum_{n=0}^{\infty}\frac{1}{(2n+1)x^{2n}}\left[2+\sum_{I=1,3,\ldots}^{\infty}\frac{1-x^2-k^2}{kx}\frac{(2n+1)(2n+2)\cdots(2n+I)}{I!}\left[\frac{k}{x}\right]^{I}\right.$$
$$\left.+2\sum_{I=2,4,\ldots}^{\infty}\frac{(2n+1)(2n+2)\cdots(2n+I)}{I!}\left[\frac{k}{x}\right]^{I}\right]$$
$$=-\sum_{n=0}^{\infty}\frac{1}{(2n+1)x^{2n}}\left[2+\sum_{I=1}^{\infty}\left[\frac{k}{x}\right]^{2I}\frac{(2n+1)(2n+2)\cdots(2n+2I)}{(2I)!}\right.$$
$$\left.\times\left[\frac{2I}{k^2(2n+2I)}(1-x^2-k^2)+2\right]\right]. \tag{17}$$

Following is the term separated from Eq. (17):

$$\sum_{I=1}^{\infty}\left[\frac{k}{x}\right]^{2I}\frac{(2n+1)(2n+2)\cdots(2n+2I)}{(2I)!}\frac{x^2}{k^2}\frac{I}{n+I}=\sum_{I=1}^{\infty}\frac{(2n+1)(2n+2)\cdots(2n+2I)}{(2I)!}\frac{I}{n+I}\left[\frac{k}{x}\right]^{2I-2}$$
$$=\frac{(2n+1)(2n+2)}{2!}\frac{1}{n+1}$$
$$+\sum_{I=2}^{\infty}\frac{(2n+1)(2n+2)\cdots(2n+2I)}{(2I)!}\frac{I}{n+I}\left[\frac{k}{x}\right]^{2I-2}$$
$$=(2n+1)+\sum_{J=1}^{\infty}\frac{(2n+1)(2n+2)\cdots(2n+2J)}{(2J)!}\frac{2n+2J+1}{2J+1}\left[\frac{k}{x}\right]^{2J}, \tag{18}$$

where $I-1$ has been substituted by J. Substituting Eq. (18) into Eq. (17) and replacing J by I yields

$$A(k,\Omega)+B(k,\Omega)=-1+\sum_{n=1}^{\infty}\frac{1}{x^{2n}}\frac{2n-1}{2n+1}-\sum_{n=0}^{\infty}\sum_{I=1}^{\infty}\frac{k^{2I}}{x^{2n+2I}}\frac{(2n+2)(2n+3)\cdots(2n+2I)}{(2I)!}\frac{I}{n+I}\left[\frac{1}{k^2}+\frac{2n(I+1)}{I(2I+1)}\right]$$
$$=-1+\sum_{n=1}^{\infty}\frac{1}{x^{2n}}\frac{2n-1}{2n+1}$$
$$-\sum_{J=1}^{\infty}\sum_{I=1}^{J}\frac{k^{2I}}{x^{2J}}\frac{[2(J-I)+2][2(J-I)+3]\cdots 2J}{(2I)!}\frac{I}{J}\left[\frac{1}{k^2}+\frac{2(J-I)(I+1)}{I(2I+1)}\right], \tag{19}$$

where J has been employed again to substitute for $n+I$. One of the terms in Eq. (19) can be revised as

$$\sum_{J=1}^{\infty}\sum_{I=1}^{J}\frac{k^{2I-2}}{x^{2J}}\frac{[2(J-I)+2][2(J-I)+3]\cdots 2J}{(2I)!}\frac{I}{J}=\sum_{J=1}^{\infty}\sum_{I'=0}^{J-1}\frac{K^{2I'}}{x^{2J}}\frac{[2(J-I')][2(J-I')+1]\cdots 2J}{[2(I'+1)]!}\frac{I'+1}{J}, \tag{20}$$

where $I'=I+1$. Separating the term given by $J=1$ and $I'=0$ and noticing that the second part of the third term of Eq. (19) contributes nothing in the case of $J=I$ yields

$$A(k,\Omega)+B(k,\Omega)=-1+\sum_{J=1}^{\infty}\frac{1}{x^{2J}}\frac{2J-1}{2J+1}-\sum_{J=1}^{\infty}\frac{1}{x^{2J}}-\sum_{J=2}^{\infty}\sum_{I=1}^{J-1}\frac{k^{2I}}{x^{2J}}\frac{[2(J-I)][2(J-I)+1]\cdots 2J}{[2(I+1)]!}\frac{I+1}{J}$$
$$-\sum_{J=2}^{\infty}\sum_{I=1}^{J-1}\frac{k^{2I}}{x^{2J}}\frac{[2(J-I)+2][2(J-I)+3]\cdots 2J}{(2I)!}\frac{2(J-I)(I+1)}{J(2I+1)}$$
$$=-1-\sum_{J=1}^{\infty}\frac{1}{x^{2J}}\frac{2}{2J+1}$$
$$-\sum_{J=2}^{\infty}\sum_{I=1}^{J-1}\frac{k^{2I}}{x^{2J}}\frac{[2(J-I)][2(J-I)+1]\cdots 2J}{(2I+1)!}\left[\frac{1}{2I+2}\frac{I+1}{J}+\frac{I+1}{J[2(J-I)+1]}\right]$$
$$=-1-\sum_{J=1}^{\infty}\frac{1}{x^{2J}}\frac{2}{2J+1}-\sum_{J=2}^{\infty}\sum_{I=1}^{J-1}\frac{k^{2I}}{x^{2J}}\frac{[2(J-I)][2(J-I)+1]\cdots[2J-1]}{(2I+1)!}\left[1+\frac{2(I+1)}{2(J-I)+1}\right]$$
$$=-1-\sum_{J=1}^{\infty}\frac{1}{x^{2J}}\frac{2}{2J+1}-\sum_{J=2}^{\infty}\sum_{I=1}^{J-1}\frac{k^{2I}}{x^{2J}}\prod_{S=1}^{2I}\frac{[2(J-I)-1+S]}{S+1}\frac{2J+3}{2(J-I)+1}, \tag{21}$$

where I' has been replaced by I. With the results of Eq. (21), the real part of dielectric function can be obtained from Eq. (14):

$$\epsilon'(\mathbf{q},\omega)=\epsilon_\infty-\frac{\alpha r_s}{2\pi k^2}\left[\sum_{J=1}^{\infty}\frac{2}{(2J+1)x^{2J}}+\sum_{J=2}^{\infty}\frac{1}{x^{2J}}\sum_{I=1}^{J-1}k^{2I}\prod_{S=1}^{2I}\frac{[2(J-I)-1+S]}{S+1}\frac{2J+3}{2(J-I)+1}\right]$$
$$=\epsilon_\infty-\frac{\alpha r_s}{2\pi k^2}C(k,x)\ , \tag{22}$$

where

$$C(k,x)=\frac{2}{3x^2}+\frac{1}{x^4}\left[\frac{2}{5}+\frac{7}{3}k^2\right]+\frac{1}{x^6}\left[\frac{2}{7}+6k^2+3k^4\right]+\frac{1}{x^8}\left[\frac{2}{9}+11k^2+\frac{77}{5}k^4+\frac{11}{3}k^6\right]+\cdots\ . \tag{23}$$

There are no large value terms left in Eq. (22), only the small value terms. This expression is very accurate in the case of small q. The curve of $C(k,x)$ in Fig. 1 shows clearly that it is the only way to yield the correct values of dielectric function in that case. The series $C(k,x)$ converges very quickly for large values of x; sometimes only the first two terms of it are needed:

$$C'(k,x)=\frac{2}{3x^2}+\frac{1}{x^4}\left[\frac{2}{5}+\frac{7}{3}k^2\right]\ . \tag{24}$$

Taking $C'(k,x)$ for $C(k,x)$ in Eq. (22), one has

$$\epsilon'(\mathbf{q},\omega)=\epsilon_\infty-\epsilon_\infty\left[\frac{\omega_p}{\omega}\right]^2\left\{1+4\left[\frac{q}{k_F}\frac{\omega_F}{\omega}\right]^2\times\left[\frac{3}{5}+\frac{7}{8}\left[\frac{q}{k_F}\right]^2\right]\right\}, \tag{25}$$

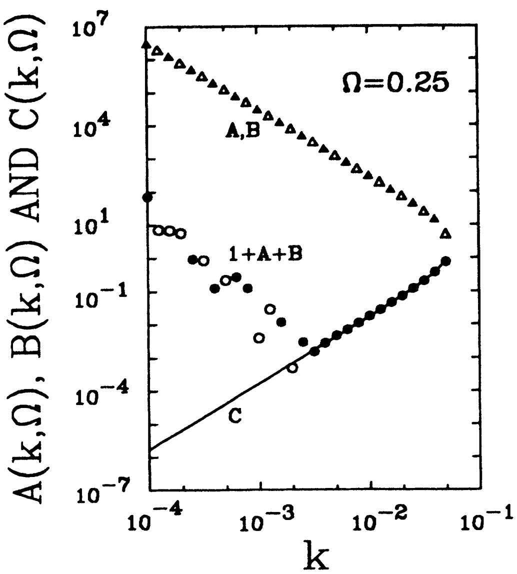

FIG. 1. The values of $A(k,\Omega)$ (△, positive), $B(k,\Omega)$ (▲, negative), and $1+A(k,\Omega)+B(k,\Omega)$ (○ for positive, ● for negative) evaluated from the analytical expression Eq. (14) and the value of $C(k,\Omega)$ (solid line) evaluated from the series expression Eq. (22) for $\omega/\omega_F=0.25$.

where

$$\frac{\alpha r^s}{2\pi k^2}\frac{2}{3x^2}=\epsilon_\infty\left[\frac{\omega_p}{\omega}\right]^2 .$$

When $q\to 0$, Eq. (25) turns out to be

$$\epsilon'(\mathbf{q},\omega)=\epsilon_\infty\left[1-\frac{\omega_p^2}{\omega^2}\right] \tag{26}$$

The plasmon dispersion relation under the approximation of Eq. (24) can then be obtained by setting $\epsilon'(\mathbf{q},\omega)=0$, namely,

$$\omega^2(q)=\omega_p^2\left[1+\frac{3}{5}\frac{v_F^2q^2}{\omega^2}\right]\simeq\omega_p^2+\tfrac{3}{5}v_F^2q^2\ , \tag{27}$$

where $E_F=\hbar\omega_F=\hbar k_F^2/2m_F^*=\frac{1}{2}m_F^*v_F$ and v_F is the velocity of carriers at the Fermi sphere. Equations (26) and (27) are the expressions frequently used in the literature, and they have appeared in textbooks.

To verify the correctness of Eqs. (22) and (25), the values of $C(k,x)$ and $C'(k,x)$ are compared in a varied frequency region, where $\omega/\omega_F=0.10$, 0.25, 0.5, and 0.75,

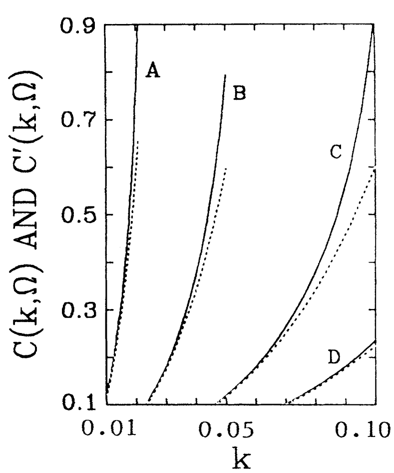

FIG. 2. The values of $C(k,\Omega)$ (solid line) and $C'(k,\Omega)$ (dashed line) given by the series expression Eq. (22) and its approximation Eq. (24), respectively, in four cases corresponding to $\omega/\omega_p=0.1$ (A), 0.25 (B), 0.5 (C), 0.75 (D), respectively.

respectively (Fig. 2). It is seen that instead of Eqs. (25) and (26), Eq. (22) should be used in infrared region.

III. HEAVY DOPING (LINEAR BAND)

It happens frequently in narrow-gap semiconductors that a conduction band can be filled by doping to such an extent that $qP \gg |E_g|$ the energy dispersion relation for most of the states is linear [Eq. (6)]:

$$E(q)=\sqrt{2/3}qP\ . \tag{28}$$

It can be obtained from Eq. (5):

$$\begin{aligned}\Delta\epsilon''_{\text{intra}}(\mathbf{q},\omega)&=\frac{e^2}{\pi q^2}\int_0^{k_F}\int_{-1}^{1}\int_0^{2\pi}(q')^2\delta((\tfrac{2}{3})^{1/2}P\{[(q')^2+q^2+2q'q\mu]^{1/2}-q'\}-\hbar\omega)dq'd\mu\, d\phi\\&=\frac{\sqrt{6}e^2}{Pq^3}\int_{-1}^{1}\int_0^{k_F}[q'k_\omega+(q')^2]\delta(\mu-\mu_0)d\mu\, dq'\\&=\frac{\sqrt{6}e^2}{Pq^3}\int_{k_2(\theta)}^{k_1(\theta)}[q'k_\omega+(q')^2]dq'\ ,\end{aligned} \tag{29}$$

where

$$k_\omega=\left[\frac{3}{2}\right]^{1/2}\frac{\hbar\omega}{P}\ ,$$

$$\mu_0=\frac{(k_\omega+q')^2-[(q')^2+q^2]}{2q'q}=\frac{k_\omega^2+2q'k_\omega-q^2}{2q'q}\ ,$$

and

$$\delta(q(\mu))=\frac{\delta(\mu-\mu_0)}{\left|\frac{d}{d\mu}g(\mu)\right|_{\mu=\mu_0}},\quad g(\mu_0)=0,\quad \left.\frac{d}{d\mu}g(\mu)\right|_{\mu=\mu_0}\neq 0\ .$$

Again, because of the confinement set by the argument of the δ function, q' and θ are no longer independent, and the integral should be carried out on a hyperbolic surface in the space inside the right Fermi sphere and outside the left Fermi surface (Fig. 7). It is known from Appendix B that (a) when $k_\omega < q$ and $0<k_\omega<2k_F-q$ (or $0<k_\omega<q<k_F$),

$$\begin{aligned}q_1'(\theta_1)&=k_F\ ,\\ q_2'(\theta_2)&=k_F-k_\omega\ ,\end{aligned} \tag{30}$$

and (b) when $0<2k_F-q<k_\omega<q$ (or $0<k_\omega<q$ and $k_F<q<2k_F$),

$$\begin{aligned}q_1'(\theta_1)&=k_F\ ,\\ q_2'(\theta_2)&=(q-k_\omega)/2\ .\end{aligned} \tag{31}$$

From Eqs. (29), (30), and (31) one has

$$\Delta\epsilon''_{\text{intra}}(\mathbf{q},\omega)=\begin{cases}\dfrac{\sqrt{6}e^2}{Pq^3}(k_F^2k_\omega-\tfrac{1}{6}k_\omega^3) & \text{when } 0<k_\omega<q<k_F\\ \dfrac{\sqrt{6}e^2}{Pq^3}[\tfrac{1}{2}k_F^2k_\omega+\tfrac{1}{3}k_F^3-\tfrac{1}{24}(2k_\omega^3-3qk_\omega^2+q^3)] & \text{when } 0<k_\omega<q \text{ and } k_F\le q<2k_F\\ 0 & \text{elsewhere}\ .\end{cases} \tag{32}$$

The real part can be obtained from Kramers-Kronig transformation:

$$\Delta\epsilon'_{\text{intra}}(\mathbf{q},\omega)=\frac{\sqrt{6}e^2}{\pi pq^3}\left\{q(2k_F^2-\tfrac{1}{3}k_\omega^2)-\tfrac{1}{9}q^3-k_\omega(k_F^2-\tfrac{1}{6}k_\omega^2)\ln\left|\frac{k_\omega+q}{k_\omega-q}\right|\right\}\ . \tag{33}$$

Equation (33) can be revised into various forms,[5] using one of which the real part of dielectric function can be written as

$$\epsilon'(\mathbf{q},\omega)=\epsilon_\infty+\tfrac{3}{2}\epsilon_\infty\left[\frac{\omega_p}{\omega y}\right]^2\left\{2-\frac{1}{9}\left[\frac{q}{k_F}\right]^2-\frac{1}{3y^2}\left[\frac{q}{k_F}\right]^2-\frac{1}{y}\left[1-\frac{1}{6y^2}\left[\frac{q}{k_F}\right]^2\right]\ln\left|\frac{1+y}{1-y}\right|\right\}\ , \tag{34}$$

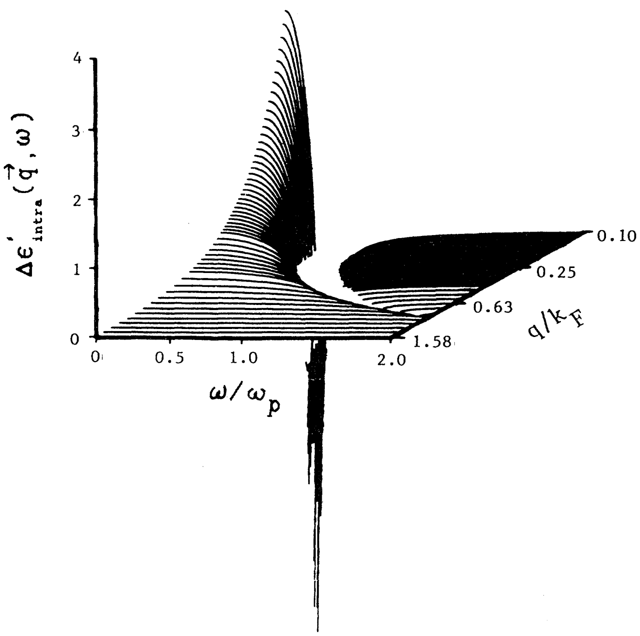

FIG. 3. The value of $\Delta\epsilon'_{\mathrm{intra}}(\mathbf{q},\omega)$ evaluated from Eq. (33) for linear band.

where $y = q/k_\omega$, and it is worthwhile to point out that in the case of a linear band the effective mass of a free carrier at the Fermi surface is

$$\frac{1}{m_F^*} = \frac{1}{\hbar^2 k_F}\frac{\partial E(q)}{\partial q} = \frac{1}{\hbar^2 k_F}\left[\frac{2}{3}\right]^{1/2} P \ . \tag{35}$$

The numerical evaluation of Eqs. (32) and (33) was performed for $k_F = 4.795\times 10^6$ cm^{-1}, $\omega_p = 676.8$ cm^{-1} and $P = 8\times 10^{-8}$ eV cm, $\epsilon_\infty = 13.01$. Figures 3 and 4 are the results shown in three-dimensional plots in the region of $\omega/\omega_p = 0$–2.0, $q/k_F = 0.1$–1.58 (real part), and 0.25–2.5 (imaginary part). It seems, at first glance, that they do not differ too much from the plots for parabolic bands. However, a detailed study will reveal an essential difference.

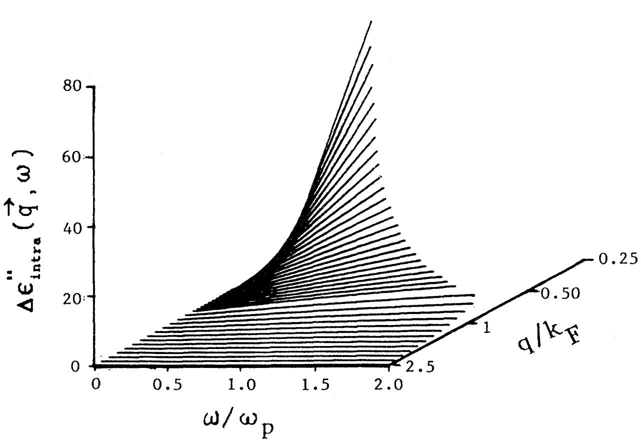

FIG. 4. The value of $\Delta\epsilon''_{\mathrm{intra}}(\mathbf{q},\omega)$ evaluated from Eq. (32) for linear band.

IV. PLASMON DISPERSION RELATION

The case of small q corresponds to the collective excitation of free carriers. For a volume plasmon, the dispersion relation can be obtained from setting the real part of the dielectric function given by Eq. (1) to zero. Numerical evaluations were performed. The parameters used in the evaluations are the same as those used in Figs. 3 and 4. In addition, $\omega_F/\omega_p = 3$ has been chosen to be the value of effective mass m_F^*.

For the parabolic band, Eq. (22) was used for the evaluation. Also, the upper boundary for electron-hole pair excitation in that case was evaluated, namely,

$$\omega(q) = \frac{E(k_F+q)-E(k_F)}{\hbar} = \frac{\hbar}{2m_F^*}(q^2+2k_F q) \ . \tag{36}$$

In the case of a linear band, Eq. (34) was used for the evaluation. The upper boundary for electron-hole pair excitation, in this case, is

$$\omega(q) = \frac{E(k_F+q)-E(k_F)}{\hbar} = \left[\frac{2}{3}\right]^{1/2}\frac{qP}{\hbar} \ . \tag{37}$$

The results are presented in Fig. 5. In the case of a parabolic band, the boundary of the pair excitation increases with q faster than the plasmon oscillation does. When $q > q_c$, a strong coupling between them takes place. As a result of the coupling, the plasmon oscillation could no longer exist. Contrary to this behavior, in the case of a linear band, the coupling between the two excitations of free carriers does not take place at all. In other words, the damping to a plasmon oscillation does not exist for the linear band, which is a unique behavior resulting

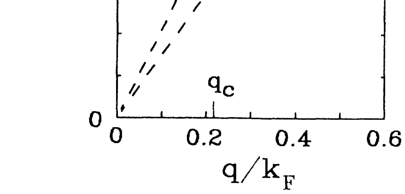

FIG. 5. The dispersion curves of plasmon oscillation [solid line, evaluated from Eq. (22) and Eq. (34)] and the up boundary of electron-hole pair excitation [dashed line, evaluated from Eqs. (36) and (37)] in semiconductors with the parabolic (P) and the linear (L) band, respectively.

from the unique energy-band dispersion relation of free carriers and has been observed experimentally.[10,11] Figure 8 presents the measured and evaluated absorption coefficients of free carriers of In-doped $Hg_{1-x}Cd_xTe$ sample T26 reported in Ref. 11. It shows evidence that with the inclusion of plasmon absorption the theory agrees with experimental results fairly well up to a frequency as high as two times that of the plasma frequency, where it was impossible for a plasmon to exist due to Landau damping. The parameters of sample T26 are composition $X=0.182$, plasma frequency $\omega_p=810$ cm^{-1}, lattice constant $a_0=6.464\times10^{-8}$ cm, frequency ν of two LO phonon modes $\nu(\mathrm{LO}_1)=137.2$ cm^{-1} and $\nu(\mathrm{LO}_2)=155.6$ cm^{-1}. It can then be evaluated ($T=295$) as follows: bandgap $E_g=0.143$ eV, free carrier concentration $N_e=6.54\times10^{18}$ cm^{-3}, and Fermi wave vector $K_F=(3\pi^2N_e)^{1/3}=5.785\times10^6$ cm^{-1}.

V. DISCUSSION

It follows from Eq. (6) that a linear band can be achieved in the case of either nearly zero gap or heavy doping. Only the latter case is within the scope of this paper.

Generally, when the appreciable plasmon effect is considered, the high density of free carriers is necessary. Because of the smallness of the effective mass, the band will become filled rather quickly as the carrier density increases. One of the limitations of $\mathbf{K}\cdot\mathbf{P}$ theory is that it is strictly valid only for the region close to the Brillouin zone center. Would doping in turn result in going beyond the zone center? Let us take sample T26 as an example to elucidate the problems. The Fermi wave vector K_F (5.785×10^6 cm^{-1}) takes only 6% of the value of $(2\pi/a_0)$ (9.721×10^7 cm^{-1}), so that we are still close enough to the zone center that the $\mathbf{K}\cdot\mathbf{P}$ theory remains valid, while the linear approximation is fairly good:

$$\tfrac{2}{3}(KP)^2=\tfrac{2}{3}[(5.785\times10^6)(8\times10^{-8})]^2=0.143\ \mathrm{eV}^2\ ,$$

$$(E_g)^2=(0.143/2)^2=0.005\ \mathrm{eV}^2\ ,$$

and obviously $(\frac{2}{3})(KP)^2 \gg (E_g/2)^2$.

The LO frequencies in most narrow-gap semiconductors are low compared with the plasma frequency in a semiconductor with a high density of free carriers. For example, the two LO modes in sample T26 are in the region of 137.2–155.6 cm^{-1}, while the plasmon oscillation is in the region higher than 810 cm^{-1}, so that their effect on carrier dynamics is negligible. On the other hand, because $E_g+E_F=0.143+0.0307=0.450$ eV, the interband

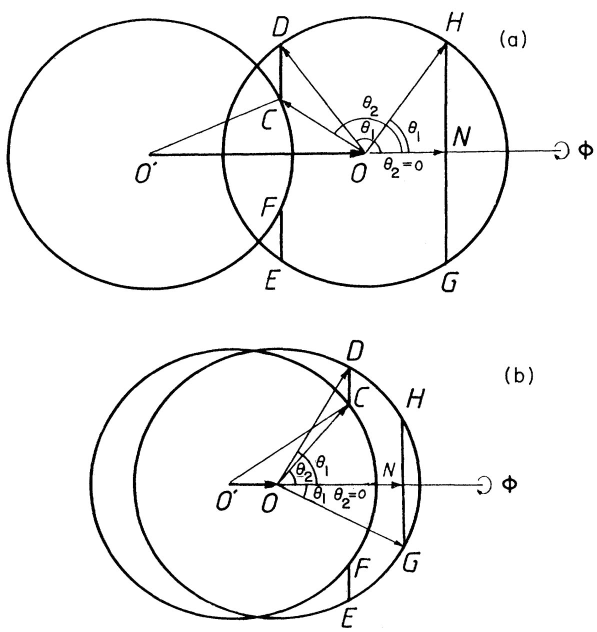

FIG. 6. The two Fermi spheres of radius k_F ($=O'C=OH=OG$) in k space separated by $\mathbf{q}$ ($=O'O$) for $k_F<q<2k_F$ (a) and $q<k_F$ (b) and the integral region in Eq. (8) described by Eq. (A2), which is a plane for semiconductors with a parabolic band. In the case of $q+\mathbf{q}'\cdot\mathbf{q}<k_F$, the region is a ring of which the cross lines in the figure plane are CD and FE, the corresponding integral limits of θ and q' are θ_1, $q_1'(\theta_1)=OD$ and θ_2, $q_2'(\theta_2)=OC$, respectively. In the case of $q+\mathbf{q}'\cdot\mathbf{q}>k_F$, the region is a disk of which the cross line in the figure plane is GH, the corresponding integral limits of θ and q' are θ_1, $q_1'(\theta_1)=OG=OH$ and $\theta_2=0$, $q_2'(\theta_2)=ON$, respectively.

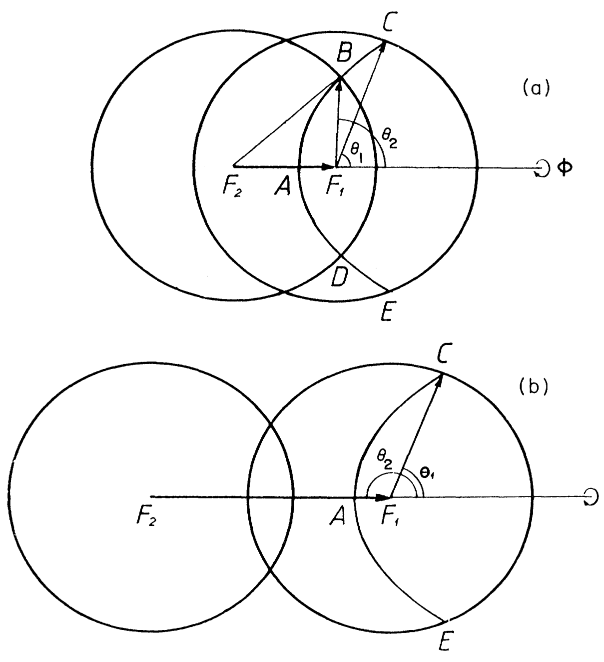

FIG. 7. The two Fermi spheres of radius k_F ($=F_2B=F_1C$) in k space separated by $\mathbf{q}$ ($=F_1F_2$), and the integral region in Eq. (29) described by Eq. (B1), which is a hyperbolic surface for semiconductors with linear band. In the case of $q-AF_1<k_F$ (a), the integral region is a belt cut from the hyperbolic surface of which the cross lines in the plane of (a) are BC and DE, the corresponding integral limits of θ and q' are θ_1, $q_1'(\theta_1)=F_1C$ and θ_2, $q_2'(\theta_2)=F_1B$, respectively. In the case of $k_F<q-AF_1<2k_F$ (b), the integral region is the top part of the hyperbolic surface of which the cross line in the plane of (b) is CAE, the corresponding integral limits of θ and q' are θ_1, $q_1'(\theta_1)=F_1C$ and $\theta_2=\pi$, $q_2'(\theta_2)=F_1A$, respectively.

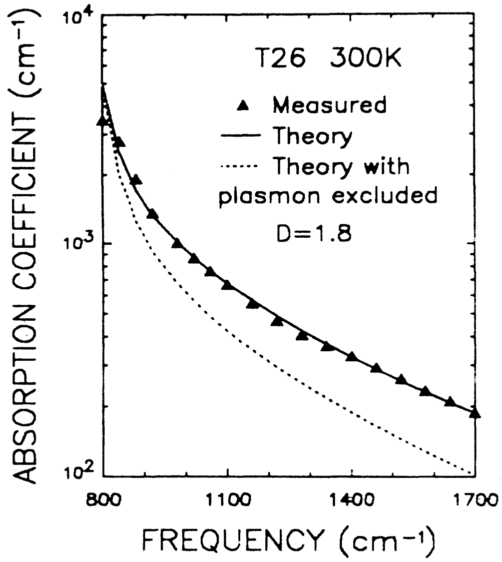

FIG. 8. The absorption coefficient of free carriers of In-doped $Hg_{1-x}Cd_xTe$ at room temperature. The plasma frequency is 810 cm^{-1}. The solid line presents the theoretical results including absorptions due to both single-carrier transitions and collective excitations with no Landau damping. The dashed line presents the theoretical results, which take into consideration only single-carrier transitions.

processes also should not take place in the region of interest, of which the highest frequency is only around 0.2 eV.

Finally, linear dispersion for conduction bands also implies linear dispersion for a light-hole band. In principle this should be accounted for in our calculation, but as a matter of fact the hole concentration is very low due to the high electron concentration, so that all hole bands involving free carrier transitions have negligible contributions.

VI. CONCLUSION

The approach developed in this paper to calculate the Lindhard function of free carriers in semiconductors with both parabolic and linear energy bands is more effective than that employed previously. In the case of the long-wavelength and infrared regions, Eq. (22), an expression of the Lindhard function in series, should be used. By virtue of doping, the degeneration could be so heavy that the energy dispersion relation of free carriers in the vicinity of Fermi surface becomes linear. This results in the unique behavior of free carriers, namely, the absence of the coupling between single-carrier transitions and the collective excitations of the carriers.

APPENDIX A: PARABOLIC BAND

The confinement equation given by the argument of the δ function in Eq. (8) is

$$\frac{\hbar^2}{2m^*}(q^2+2q'q\cos\theta)-\hbar\omega=0 \ . \tag{A1}$$

Equation (A1) can be revised as

$$\mathbf{q}'\cdot\mathbf{q}_0=\frac{q_\omega^2-q^2}{2q} \ , \tag{A2}$$

where $\mathbf{q}_0=\mathbf{q}/q$, $q_\omega^2=2m^*\omega/\hbar$.

For the given q and ω, Eq. (A2) describes where the integral in Eq. (8) should be performed. It is a plane in between the two Fermi spheres in the shape of a disk or ring (Fig. 6) depending on where the plane is located, which is determined by k_F, q, and ω.

(a) $q+\mathbf{q}'\cdot\mathbf{q}<k_F$, the integral is to be performed on a ring, and one has

$$q_1'(\theta_1)=k_F \ . \tag{A3}$$

$q_2'(\theta_2)$ can be calculated from $\Delta O'OC$:

$$k_F^2=[q_2'(\theta_2)]^2+q^2-2q_2'(\theta_2)q\cos(\pi-\theta_2)=[q_2'(\theta_2)]^2+q_\omega^2 ,$$
$$[q_2'(\theta_2)]^2=k_F^2-q_\omega^2 \ . \tag{A4}$$

(b) $q+\mathbf{q}'\cdot\mathbf{q}>k_F$, the integral is to be performed on a disk, and one has

$$q_1'(\theta_1)=k_F \ , \tag{A5}$$

$$q_2'(\theta_2)=\mathbf{q}'\cdot\mathbf{q}_0=\frac{q_\omega^2-q^2}{2q}=\frac{m^*\omega}{\hbar q}-\frac{q}{2} \ . \tag{A6}$$

APPENDIX B: LINEAR BAND

The confinement equation given by the argument of the δ function in Eq. (29) is

$$q'=\frac{q^2-k_\omega^2}{2k_\omega[1-(q/k_\omega)\cos\theta]}=\frac{p}{1-e\cos\theta} \ , \tag{B1}$$

where $p=(q^2-k_\omega^2)/2k_\omega$, $e=q/k_\omega$, and $k_\omega=\sqrt{3/2}(\hbar\omega/p)$.

In order for p to be positive, q should be greater than k_ω so that $e>1$. This is always correct in the infrared region, so that Eq. (B1) defines a hyperbolic surface (Fig. 7).

(a) $0<q-AF_1<k_F$ (equivalent to $k_\omega<q$ and $0<k_\omega<2k_F-q$ or $0<k_\omega<q<k_F$), and the integral is to be performed on the belt cut from the hyperbolic surface of which the cross curves in the figure plane are BC and DE. It is obvious that

$$q_1'(\theta_1)=k_F \ . \tag{B2}$$

$q_2'(\theta_2)$ can be calculated from ΔF_2F_1B:

$$k_F^2=[q_2'(\theta_2)]^2+q^2-2q_2'(\theta_2)q\cos(\pi-\theta_2) \ . \tag{B3}$$

Substituting Eq. (B1) into Eq. (B3) yields

$$q_2'(\theta_2)=k_F-k_\omega \ . \tag{B4}$$

(b) $0<k_F<q-AF_1$ and $k_F<q<2k_F$ (equivalent to $0<2k_F-q<k_\omega<q$ or $0<k_\omega<q$ and $k_F<q<2k_F$) and the integral is to be performed on the hyperbolic surface of which the cross curve in the plane is CAE. It is obvious that

$$q_1'(\theta_1)=k_F \ , \tag{B5}$$

$$q_2'(\theta_2)=\frac{ep}{e^2-1}-\frac{p}{e^2-1}=\frac{p}{e+1}=\frac{q^2-k_\omega^2}{2k_\omega}\frac{k_\omega}{q+k_\omega}=(q-k_\omega)/2 \ . \tag{B6}$$

[1]E. O. Kane, J. Phys. Chem. Solids **1**, 249 (1957).

[2]J. Lindhard, K. Dan. Vidensk. Selsk., Mat. Fys. Medd. **28**, 8 (1954).

[3]J. Ziman, *Principles of the Theory of Solids* (Cambridge University Press, Cambridge, 1972).

[4]W. Szuszkiewicz, A. M. Witowski, and M. Grynberg, Phys. Status Solidi B **87**, 637 (1978).

[5]W. Szuszkiewicz and W. Bardyszewski (unpublished).

[6]C. Kittel, *Introduction to Solid State Physics,* 5th ed. (Wiley, New York, 1976).

[7]A. Ron and N. Tzoar, Phys. Rev. **131**, 1943 (1963).

[8]J. P. Walter and M. L. Cohn, Phys. Rev. B **5**, 3101 (1972).

[9]M. E. Kim, A. Das, and S. D. Senturia, Phys. Rev. B **18**, 6890 (1978).

[10]W. Szuszkiewicz, Qian Dingrong, and K. Karpierz, Acta Phys. Pol. A **73**, 357 (1988).

[11]Qian Dingrong, W. Szuskiewicz, Zhang Jiaming, and W. Bardyszewski, in *Proceedings of the 19th International Conference on the Physics of Semiconductors, Warsaw, Poland, 1988,* edited by W. Zadwadzki (Institute of Physics, Polish Academy of Science, Warsaw, 1988), p. 1715.